JZUS A

Characteristics of interior noise of a Chinese high-speed train under a variety of conditions[*]

Jie ZHANG, Xin-biao XIAO, Xiao-zhen SHENG[†‡], Rong FU, Dan YAO, Xue-song JIN

(*State Key Laboratory of Traction Power, Southwest Jiaotong University, Chengdu 610031, China*)

[†]E-mail: shengxiaozhen@hotmail.com

Abstract: This paper presents an investigation into the characteristics of interior noise of a Chinese high-speed train under several typical conditions. Interior noises within Vehicle TC01, which can be used as a head car or an end car, and Vehicle TP03, the third car counting from TC01, are measured for the train running at speeds from 260 km/h to 385 km/h, along two types of track including a slab track and a ballast track and either on the ground surface or in a tunnel. Data analyses are performed for sound pressure overall levels, frequency, area contributions, and possible generation mechanisms, showing how they are affected by train speed, running direction, track type, and tunnel. The results show that, whether TC01 is used as head car or end car, the interior noise characteristics in the VIP cabin are mostly related to aerodynamic noise. Differences in interior noise between tracks become smaller as the train speed increases. The effect of a tunnel on the interior noise is more important for the middle coach than that for the head coach. This study can provide a basis for noise control of high-speed trains.

Key words: High-speed train; Interior noise; Noise source identification; Contribution analysis; Various conditions; Noise characterization

http://dx.doi.org/10.1631/jzus.A1600695   **CLC number:** U270.16

1 Introduction

With the increase of the train speeds, interior noise is becoming a key issue for operating high-speed railways (Jin, 2014). Over the past decades, there has been a significant amount of research on interior noise, such as source mechanism investigation (Frémion *et al*., 2000; Thompson and Jones, 2000; Thompson and Gautier, 2006; Zhang *et al*., 2014), transfer path analysis (Eade and Hardy, 1977; Fan *et al*., 2014; Ström, 2014), and interior noise evaluation

(Hardy, 2000; Létourneaux *et al*., 2000; Kuwano *et al*., 2004). However, the interior noises of a train, running at different speeds, on different types of track, and inside and outside a tunnel, are quite different, requiring different noise control methods according to different special noise characteristics. Therefore, it is important to study interior noise of high-speed trains under a variety of conditions. Soeta and Shimokura (2013) researched the effects of noise sources on the interior noise characteristics in a number of types of trains. They found that compared with wheel/rail rolling noise, impact noise had larger components at frequencies below 500 Hz, while curve squeal noise had larger components at frequencies between 125 Hz and 500 Hz. Shin and Park (2003) analyzed the flow field around a high-speed train entering a tunnel by applying a 3D unsteady Navier-Stokes equation solver. Based on numerical study, it was found that the pressure in the nose region was significantly

increased due to piston-like action when the train was just at the tunnel entrance. Park *et al.* (2015) measured the noise in passenger compartments of high-speed trains operating in Korea under various conditions, and proposed a new method to quantify the annoyance based on a number of sound quality metrics. They found that the annoyance under sudden noise change using level-equalized sounds had a high correlation with the maximum gradient value of the sharpness.

However, compared to research on the exterior noise of high-speed trains (Mellet *et al.*, 2006; He *et al.*, 2014), there is still a large potential for study on interior noise. This paper presents an investigation on the characteristics of interior noise of a Chinese high-speed train under several typical conditions. Interior noises are measured for the train to run at speeds from 260 km/h to 385 km/h including two running directions, along two types of track including a slab track and a ballast track, and either on the ground surface or in a tunnel. In this paper, we first introduce the measurement configurations including measured train type, test conditions, and measurement points. Then, a data processing and analysis flowchart is shown and explained. At last, the approach is applied to identify the interior noise characteristics and area contributions.

2 Measurement configurations

2.1 Description of measured train type and test conditions

The high-speed train consists of eight coaches. Interior noise is measured in the first and the third coaches. The first coach, numbered TC01, is a trailer car having a driver's cab and a VIP cabin, and the third coach, numbered TP03, is also a trailer car but with a pantograph on the roof of one of the coach ends. Test conditions or cases are summarized in Table 1. Measurements are performed for interior noise and interior noise source identification.

It must be noted that, for case 1, when investigating the effect of train speed on interior noise, the interior noises are only tested in TC01, and the interior noise source identification is only tested in the VIP cabin. For case 2, while examining the effect of track types on interior noise, the interior noises are

only tested in TP03, and the interior noise source identification is only tested at the coach end. For case 3, when investigating the effect of tunnel on interior noise, although the interior noises are tested both in TC01 and TP03, there are no interior noise source identification results. The above inconsistency is due to limitations in the experimental conditions.

2.2 Measurement points of interior noise

Fig. 1 shows the measurement points of the interior noise. There are six microphones positioned in the driver's cab (N1), the VIP cabin (N2), and at the coach end (N3) of TC01, and in the front (N4), the middle (N5), and at the end (N6) of TP03. Here N6 is under the pantograph. All the microphones (B&K Type 4190) are positioned at a height of 1.2 m above the interior floor. Fig. 2 shows the photograph of the interior noise measurement.

The noise measurement was conducted using a B&K PULSE platform and 32 768 Hz sampling frequency. All transducers had been calibrated before the test.

2.3 Interior noise source identification

Interior noise source identification is carried out using a spherical microphone array (B&K WA1565W004). A sound pressure field is denoted by $p(k, r, \Omega)$, where k is the acoustic wave number, and $(r, \Omega) \equiv (r, \theta, \phi)$ is the spatial location in spherical coordinates (Williams, 1999; Cohen *et al.*, 2010). The spherical Fourier transform of the pressure is given by (Williams, 1999)

$$p_{nm}(k, r) = \int_{\Omega \in S^2} p(k, r, \Omega) Y_n^{m*}(\Omega) \mathrm{d}\Omega, \qquad (1)$$

with the inverse transform relation

$$p(k, r, \Omega) = \sum_{n=0}^{\infty} \sum_{m=-n}^{n} p_{nm}(k, r) Y_n^m(\Omega), \qquad (2)$$

where $\int_{\Omega \in S^2} \mathrm{d}\Omega \equiv \int_0^{2\pi} \int_0^{\pi} \sin\theta \mathrm{d}\theta \mathrm{d}\phi$, which covers the entire surface area of the unit sphere denoted by S^2 (S^2 is the space defined in a sphere of constant radius), and $Y_n^m(\Omega)$ is the spherical harmonics of order n and degree m (Williams, 1999):

Table 1 Test conditions of the interior noise

Case	Coach	Speed (km/h)	Track	Line	Direction of TC01
1	TC01	260/280/300/310 320/330/350/385	Slab	On the ground surface	Head/End
2	TP03	200/250	Ballast/Slab	On the ground surface	Head
3	TC01/TP03	300/350	Slab	On the ground surface/In a tunnel	Head
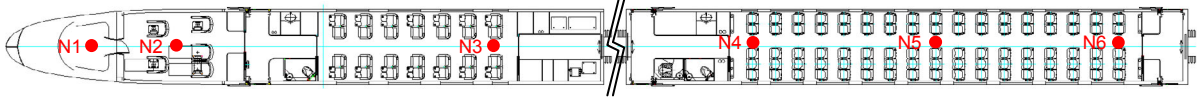
Fig. 1 Measuring points in the two coaches of a high-speed train ("●" refers to acoustic measurement point)

Fig. 2 Photograph of the interior noise measurement

$$Y_n^m(\Omega) \equiv \sqrt{\frac{(2n+1)}{4\pi}\frac{(n-m)!}{(n+m)!}} P_n^m(\cos\theta)\mathrm{e}^{\mathrm{i}m\phi}, \qquad (3)$$

where $\mathrm{i} = \sqrt{-1}$ and $P_n^m(\cdot)$ is the associated Legendre function.

A sound field composed of a single plane wave is of great importance for beam forming because beam patterns are typically measured as the array response to a single plane wave. Therefore, considering a sound field composed of a single plane wave of amplitude $a(k)$, with an arrival direction Ω_0, p_{nm} can be written as (Rafaely, 2004)

$$p_{nm}(k,r) = a(k)b_n(kr)Y_n^{m*}(\Omega_0), \qquad (4)$$

where $b_n(kr)$ depends on the sphere boundary and reads

$$b_n(kr) = \begin{cases} 4\pi\mathrm{i}^n\left[j_n(kr) - \dfrac{j_n'(kr_{\mathrm{a}})}{h_n'(kr_{\mathrm{a}})}h_n(kr)\right], & \text{rigid sphere,} \\ 4\pi\mathrm{i}^n j_n(kr), & \text{open sphere,} \end{cases} \qquad (5)$$

where j_n and h_n are the spherical Bessel and Hankel functions, and j_n' and h_n' are their derivatives, respectively; r_{a} is the radius of the rigid sphere.

Fig. 3 shows the photograph of the interior noise source identification. The spherical microphone array is made up of 50 microphones and 12 cameras, and the diameter of the array is 19.5 cm, acoustically much smaller than the dimensions of the coach. It is positioned with its center at the same point as the microphone indicated in Fig. 1.

Fig. 3 Photograph of the interior noise source identification

3 Data processing and analysis flowchart

3.1 Approach of data processing

Different running conditions affect not only exterior sources, but also sound transfer paths, and therefore interior noise. For the purpose of noise control and low-noise design of high-speed trains, measured data must be processed and analyzed properly and adequately. A data processing and analysis flowchart is shown in Fig. 4.

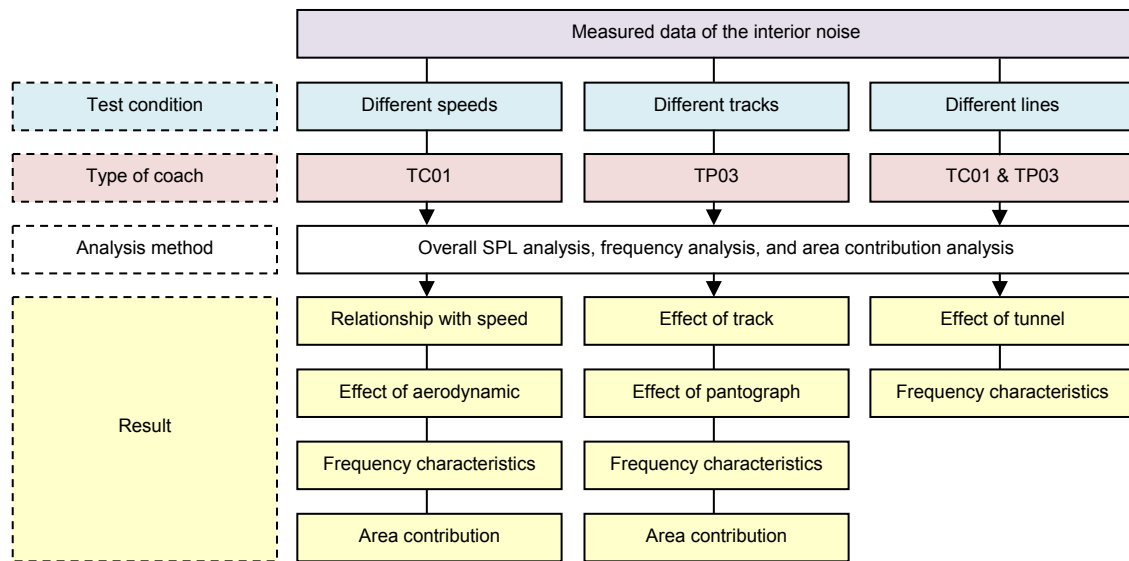Test conditions can be grouped into three sets: different speeds, different tracks, and different lines.

Fig. 4 Approach of data processing (SPL is sound pressure level)

For the first set of conditions, TC01 is examined. For the second set of conditions, TP03 is the object. Finally, for the last set of conditions, both TC01 and TP03 are selected as research objects. The measured data of the interior noise are analyzed in terms of overall sound pressure level (SPL), frequency component, and area contribution.

For different speeds, the relationship between the overall SPL and the train speed is investigated. According to the characteristics of overall SPL in TC01 when it was used as head car and end car, respectively, the effect of aerodynamic noise on the interior noise is obtained. Through frequency contribution analysis, dominant frequencies of aerodynamic noise are discovered. Finally, area contribution analysis can help us to identify where the noise comes from.

For different tracks, through overall SPL analysis of the two measured points above the two bogies (one of the points is under the pantograph), the effect of the rack and the effect of the pantograph on the interior noise are obtained. The dominant frequencies of the slab track and the ballast track are discovered through frequency analysis. Finally, the area contribution of the ballast track is discussed.

For different lines, according to the characteristics of the overall SPL and frequency domain, the effect of tunnel on the interior noise and the difference of frequencies between on the ground surface and in a tunnel are investigated.

3.2 Treatment of the measured data

Because of the limitation of the experimental conditions, only one test is performed for each case. However, for each test, measurement is carried out with the train running at a constant speed for about 30 s over a distance of about 2 km. This means that, during each test, the train can be assumed to be unchanged and excitation to the train can be assumed to be a representative stable stochastic process. Thus, the measured data can provide statistics which are of sufficiently high statistical significance. Moreover, all the noise data are analyzed by using the software B&K PULSE. Each result shown in this paper is the average of results of data sections of 1 s with 66.67% overlap. This data processing will largely average out the random measurement noise. A-weighting is used as acoustic weighting, and exponential averaging, with a time constant of 1/8 s which is also called "fast" averaging, is used as time weighting. According to the theoretical manual of B&K PULSE, for the noise spectrum estimate, 6-pole filters are used with center frequencies as

$$f_c = 10^{(n/10)}, \tag{6}$$

where $17 \leq n \leq 37$. The 21 filters allow lower and upper center frequencies from 50 Hz to 5 kHz. The average of a random signal is an estimation of the true (RMS-power) value with an error interval given by

$$\pm\varepsilon = \frac{1}{2 \times \sqrt{BT_A}}, \quad BT_A \gg 1, \tag{7}$$

where B is the filter bandwidth, and T_A is the averaging time.

4 Results and discussion

4.1 Effect of train speed on interior noise

According to the relationship between exterior noise levels and speeds of high-speed trains (Mellet *et al.*, 2006; He *et al.*, 2014), when the value of $L_p(v_0)$ at the reference speed v_0 is known, the linear regression law can be expressed as

$$L_p(v) = a \lg(v/v_0) + L_p(v_0), \tag{8}$$

where a is a coefficient, L_p is the sound pressure level, and v is the train speed. The linear regressions for different measurement points between interior noise and speed are obtained from Eq. (8).

Fig. 5 shows the interior noise levels of TC01 when it was used as head car running along a slab track, while Fig. 6 shows results when it was used as end car. The horizontal axis represents train speed in logarithmic scale.

4.1.1 Sound pressure overall levels of interior noise in TC01 as head car

From Fig. 5 it can be seen that, when TC01 is used as head car running from 260 km/h to 385 km/h, the interior noises regression coefficients (i.e., a in Eq. (8)) for the three measurement positions N1, N2, and N3 are 58.00, 56.12, and 53.10, and the corresponding correlation coefficients R^2 are 0.96, 0.88, and 0.95, and the P-values are 8.9213×10^{-6}, 3.5010×10^{-4}, and 1.9841×10^{-5}, respectively.

The noise levels in the driver's cab, in the VIP cabin, and at the coach end all increase with speed, as expected. However, the increase rate becomes smaller as the measurement point moves away from the train nose (or towards the end of the coach). On average, interior noise in the driver's cab is about 3 dBA higher than that in the VIP cabin or at the coach end. On the one hand, according to the train pass-by noise characteristics (Mauclaire, 1990; Krylov, 2001; He *et*

al., 2014), when below the dividing speed, wheel/rail rolling noise is dominant, and the slope of the linear function of exterior noise is approximately 30; while above the dividing speed, aerodynamic noise is dominant, and the slope becomes 60. It can be suggested that when TC01 is used as head car, the interior noise in the driver's cab must be aerodynamically dominated, since the rate (58.00) of dependence on train speed is close to 60. While on the other hand, the driver's cab is just behind the wind screen of the train nose, and the sound insulation of the wind screen is lower than that of the car body.
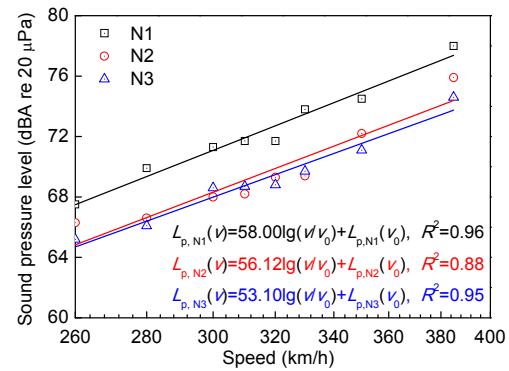
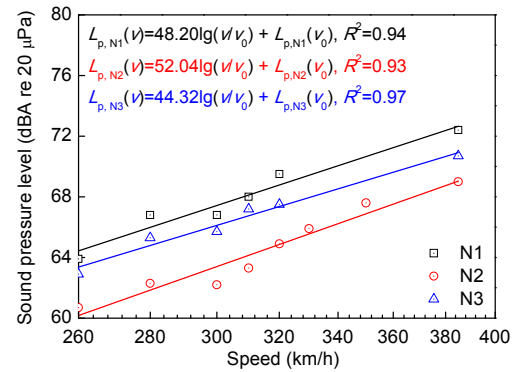**Fig. 5 Interior noise levels at different speeds (head car)**

Fig. 6 Interior noise levels at different speeds (end car)

Interior noise in the VIP cabin is slightly less than 1 dBA higher than that of the coach end, and the difference between them becomes even smaller as train speed decreases. This is because both positions are immediately above a bogie and therefore mainly affected by noise and vibration around the bogie area, including wheel/rail rolling noise, bogie aerodynamic noise, and bogie vibration. However, the rate of dependence on train speed in the VIP cabin is higher by

a factor of 3 than that of the coach end, and this can be explained by the fact that the aerodynamic noise generated by the first bogie always has a higher source level than that of the other bogies (Mauclaire, 1990; Krylov, 2001; He *et al*., 2014).

4.1.2 Sound pressure overall levels of interior noise in TC01 as end car

Two observations can be made from Fig. 6. The first is that, when TC01 is used as end car, the interior noise regression coefficients for the three measurement points became 48.20, 52.04, and 44.32, and the *P*-values are 8.4281×10^{-4}, 5.7753×10^{-5}, and 2.7502×10^{-4}, respectively. The interior noise regression coefficients decreased by about 10 for both the driver's cab and the coach end, but only by 4 for the VIP cabin, from the head car case. As mentioned in Section 4.1.1, the decrease of the interior noise regression coefficients suggests that, when TC01 is used as end car, the contribution from aerodynamic noise becomes less dominant than when it is used as head car. However, since the interior noise regression coefficient decreases only by 4 for the VIP cabin, the interior noise in the VIP cabin is still more related to aerodynamic noise than the other two positions even when it runs as end car. The second observation is that, when TC01 was run as end car, the SPLs of the driver's cab, the VIP cabin, and the end of the coach are reduced by an average of 3.8, 5.0, and 2.1 dBA, respectively, making the interior noise in the VIP cabin the lowest. According to the exterior noise source identification results of Chinese high-speed trains (He *et al*., 2014), it is due to the fact that the noise around the last bogie is the lowest. Why the last bogie is the quietest is a to-be-answered question.

4.1.3 Frequency spectrum analysis for interior noise in the VIP cabin

The main difference of source between TC01 run as head car and end car is aerodynamic noise. In order to investigate the effect of aerodynamic noise on interior noise, we take the VIP cabin at 350 km/h as an example. Fig. 7 shows the noise spectrum in 1/3 octave bands with TC01 as both head car and end car. The left vertical axis indicates the SPL of the VIP cabin and the right one indicates their difference in SPL between "head car" and "end car".

From Fig. 7 it can be seen that the shape of the sound pressure spectrum in the VIP cabin (at N2) when TC01 is used as head car is similar to that when it is used as end car. They both have peaks in 1/3 octave bands centered at 200 Hz and 630 Hz. However, when TC01 is used as head car, the spectrum is higher than when it is used as end car for all central frequencies except 630 Hz. Because the difference in test condition for the interior noise measurement and source identification in the VIP cabin is the train's running direction only, the wheel/rail rolling noise would not be changed. It is suggested that the differences of the interior noise spectra are caused by aerodynamic noise. Moreover, as the mean difference of the interior noise spectra in the VIP cabin between "head car" and "end car" is 3.7 dBA, it can be further concluded that the dominant frequency difference caused by aerodynamic noise is the 1/3 octave bands centered from 63 Hz to 315, 2000, and 2500 Hz. Furthermore, for the 1/3 octave band centered at 630 Hz, the noise level is almost unchanged whether TC01 is used as head car or end car. That is to say, the difference of aerodynamic noise caused by different running directions has little influence on this frequency band. For high speeds, especially the 350 km/h in this paper, wheel/rail rolling noise and aerodynamic noise are the two most dominant sources (Mellet *et al*., 2006). In another words, the 1/3 octave band centered at 630 Hz must be more related to wheel/rail rolling noise or bogie vibration.

4.1.4 Sound pressure contribution analysis for interior noise in the VIP cabin

Figs. 8 and 9 show contributions of different frequency bands to the total sound pressure in the VIP cabin for different speeds when TC01 is used as head car (Fig. 8) and end car (Fig. 9). The frequency band contributions are calculated by

$$\alpha_{i\text{th band}} = \left(p_{i\text{th band}}^2 \middle/ \sum p_{i\text{th band}}^2 \right) \times 100\%, \qquad (9)$$

where $p_{i\text{th band}}$ is the equivalent sound pressure in the *i*th 1/3 octave band.

From Fig. 8, when TC01 was used as head car running at different speeds, the top three contributors are 1/3 octave bands centered at 125, 160, and 200 Hz. The contributions of the 1/3 octave bands centered at
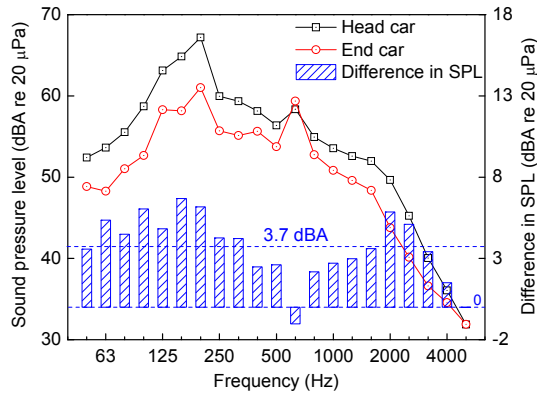
Fig. 7 Comparison of the interior noise in the VIP cabin between TC01 as head car and end car (350 km/h)
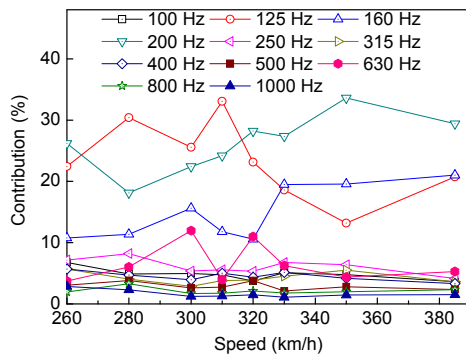

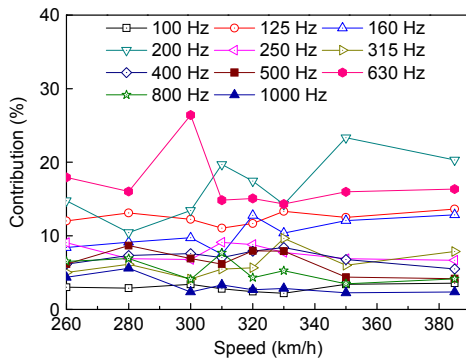**Fig. 8 Sound pressure contribution at different speeds (as head car)**

Fig. 9 Sound pressure contribution at different speeds (as end car)

160 and 200 Hz increase with train speed, but those of the 1/3 octave band centered at 125 Hz decrease with train speed. Therefore, the noise contribution distributions in frequency domain are train speed-dependent. Moreover, because the interior noise in the VIP cabin is more related to aerodynamic noise, as

mentioned in Sections 4.1.1 and 4.1.2, and aerodynamic noise of high-speed trains generally is low frequency dominant (Frémion *et al.*, 2000), the 1/3 octave bands centered at 125, 160, and 200 Hz are mainly from an aerodynamic contribution.

From Fig. 9, when TC01 is used as end car, the interior noises in the 1/3 octave band centered at 630 Hz have high contributions to the overall SPLs at each speed, especially 300 km/h, at which the contribution rate reached 26%. Furthermore, at speeds above 300 km/h, the contribution rate in the 1/3 octave band centered at 200 Hz is gradually raised and becomes dominant. It is further indicated that, although TC01 was used as end car, there is a great effect of aerodynamic noise on the interior noise of the VIP cabin especially when the train speed is high.

Both in Figs. 8 and 9, the contributions in most 1/3 octave bands are below 10% except those centered at 125, 160, 200, and 630 Hz. It can be concluded that whether TC01 is used as head car or end car, the most important noise frequencies in the VIP cabin are the above four 1/3 octave bands.

4.1.5 Area contribution analysis for interior noise in the VIP cabin

Fig. 10 shows the noise source identification result in the VIP cabin. The range of sound intensity contour is 3 dBA. The train was running at 350 km/h and TC01 ran as head car.

From Fig. 10, the overall source in the VIP cabin is mainly located on the roof and the floor. In order to further obtain the area contribution in different frequencies to the overall source, first, the VIP cabin is divided into six areas, i.e., the roof, the left sidewall, the right sidewall, the floor, the front, and the rear of the cabin, as shown in Fig. 11.

The sound intensity integral in each area is produced to give the sound power for this area. Then, the noise source contribution of the areas is calculated by

$$\alpha_{i\text{th band},\,j\text{th source}} = \frac{W_{i\text{th band},\,j\text{th source}}}{\displaystyle\sum_{\text{bands}}\sum_{\text{sources}} W_{i\text{th band},\,j\text{th source}}} \times 100\%, \quad (10)$$

where $W_{i\text{th band},\,j\text{th source}}$ is the sound power of the ith 1/3 octave band and the jth area.
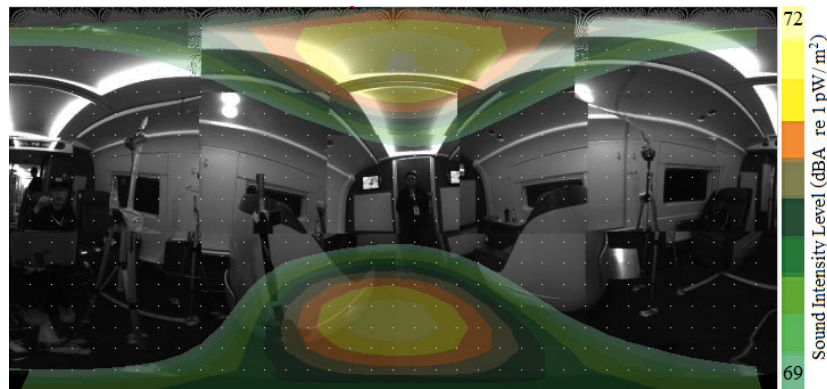
Fig. 10 Noise source identification result in the VIP cabin (50–5000 Hz)
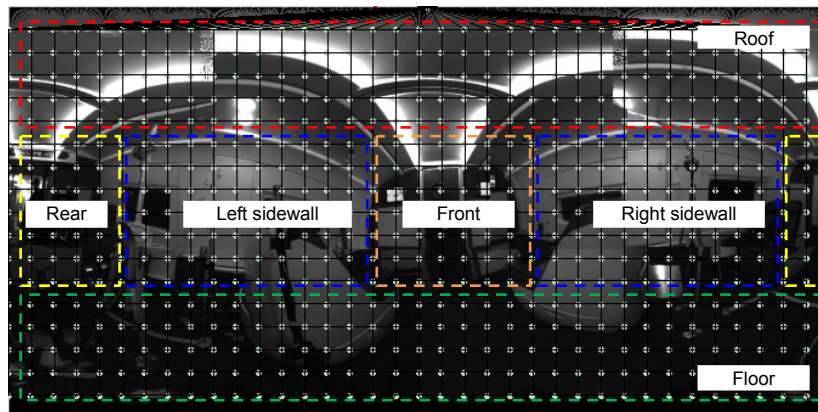

Fig. 11 Divided areas of the VIP cabin

Fig. 12 shows the overall source spectrum and the area contributions in different 1/3 octave bands. From Fig. 12, the dominant overall sources are in the 1/3 octave bands centered from 100 Hz to 200 Hz, and the main contributing areas are the roof and the floor. Moreover, there is a peak of the overall source in 1/3 octave band centered at 630 Hz. The area contributions in this band from high to low are the floor, the right sidewall, the roof, and the left sidewall in turn, and their contribution rates are 24.7%, 20.2%, 16.3%, and 15.9%, respectively.

4.2 Effect of track types on interior noise

4.2.1 Sound pressure overall levels of interior noise in TP03

Fig. 13 shows the interior noise levels at N4–N6 in TP03 when the train ran along a slab track and a ballast track, both having similar rail roughness levels. Some differences between the slab track and the ballast track are identified: (1) railpad stiffness for the slab track is around 20–30 kN/mm while that of the

ballast track is much higher, about 60–70 kN/mm; (2) ballast provides sound absorption while the slab does not; (3) both sleepers in the ballast track and slabs in the slab track radiate sounds at low frequencies, but the former has a much smaller radiation area than the latter. Tested train speeds were 200 and 250 km/h, with TC01 as head car. The measurement point N6 is under a pantograph.

From Fig. 13 it can be seen that, when the train ran at 200 km/h along the slab track, the interior noise level in the front of the coach (at N4) is 2.5 dBA higher than that when the train ran on the ballast track at the same speed. At 250 km/h, this difference decreases to 1.4 dBA. Measurement point N4 is just above the front bogie of the coach. It can be seen that the ballast track has an effect of reducing noise at that point.

In the middle of the coach (at N5), when the train was running at 200 km/h along the slab track, the interior noise level is 0.8 dBA higher than that on the ballast track. At 250 km/h, this difference is 0.7 dBA.
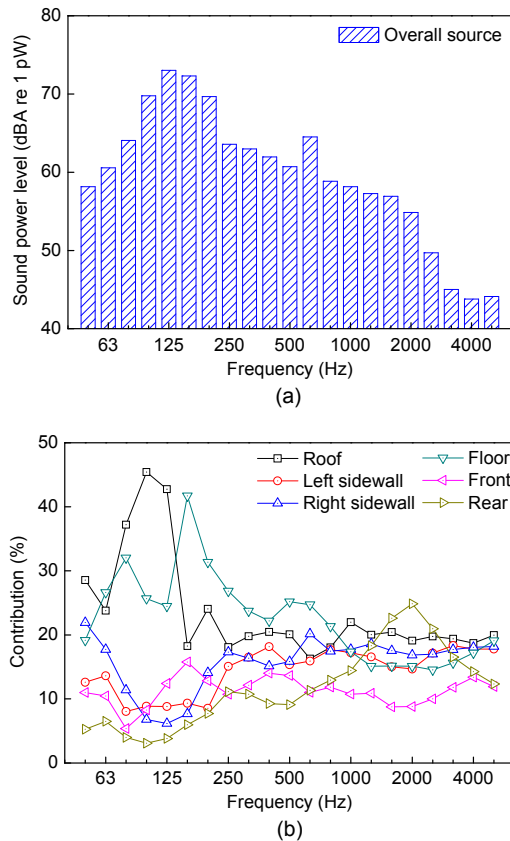
Fig. 12 Area contributions in 1/3 octave band spectrum in the VIP cabin: (a) overall source spectrum; (b) area contributions in different 1/3 octave bands
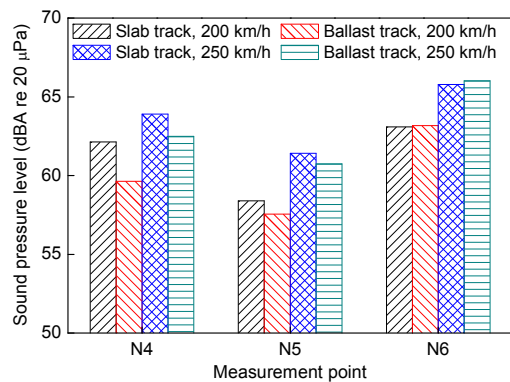

Fig. 13 Interior noise levels on different tracks

At the end of the coach (at N6) just below the pantograph, there is almost no difference in interior noise levels between the slab track and the ballast track. Both measurement points N4 and N6 are immediately above a bogie, but the point N6 is also below a pantograph, so the interior noise at N6 is more affected by pantograph noise and vibration

rather than wheel/rail rolling noise and bogie vibration.

From the above we note that differences in interior noise between the slab track and the ballast track are train speed-dependent. The higher the speed is, the smaller the difference is. It is because when the speed increases, aerodynamic load becomes dominant so that the difference of wheel/rail rolling noise and bogie vibration caused by different tracks becomes secondary.

4.2.2 Frequency spectrum analysis for interior noise of TP03

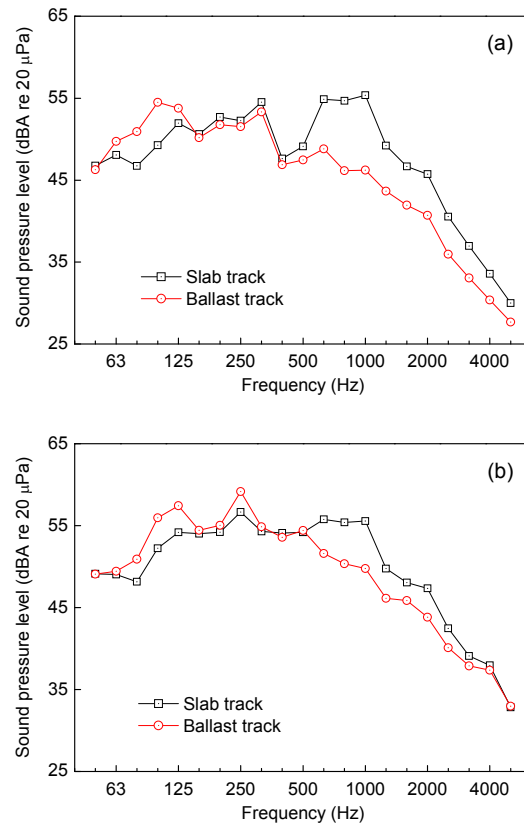Fig. 14 shows the noise spectrum in 1/3 octave bands on different tracks at 250 km/h.

Fig. 14 Interior noise spectra on different tracks at points N4 (a) and N6 (b) (250 km/h)

Note that the overall level at N4 when the train ran along the slab track at 250 km/h is only 1.4 dBA higher than when it is on the ballast track. This is reflected in the spectrum of interior noise at that point. It is seen from Fig. 14a that, for frequencies lower

than 125 Hz, the noise levels for the ballast track are higher than those for the slab track. This is related to the fact that the slab track has much smaller railpad stiffness than the ballast track. As a result, slabs in the slab track vibrate less than the sleepers in the ballast track, and radiate less sound. However, when frequencies are higher than 500 Hz, the ballast track behaves much better than the slab track. This is because, on the one hand, the rail in the ballast track has lower vibration and a higher vibration decay rate than those in the slab track due to difference in railpad stiffness, and on the other hand, at sufficiently high frequencies, the ballast can absorb some sound from the rail (Zhang *et al*., 2016; Sheng *et al*., 2017). For other frequencies, these two tracks perform similarly. Therefore, the differences of the interior noise frequencies caused by different tracks are mainly the 1/3 octave bands centered lower than 125 Hz and higher than 630 Hz.

At measurement point N6, although the overall levels are almost the same for the two tracks, the frequency spectra are different to some extent. It is seen from Fig. 14b that, for frequencies lower than 250 Hz, the noise levels for the ballast track are higher than those for the slab track. However, when frequencies are higher than 630 Hz, the ballast track produces less noise than the slab track. Nevertheless, at N6, both on the slab and ballast, there is a peak in 1/3 octave band centered at 250 Hz. This is the reason why there is little difference in the overall levels between these two tracks under a pantograph. It is indicated that when the train runs at 250 km/h, 1/3 octave band centered at 250 Hz is one of the dominant frequency bands of pantograph noise.

4.2.3 Area contribution analysis for interior noise of TP03

Fig. 15 shows the noise source identification result at the coach end of TP03 (i.e., measurement point N6). The range of the sound intensity contour is 3 dBA. The train was running at 250 km/h on the ballast track.

From Fig. 15, the overall source at the end of the coach is mainly located on the roof and the sidewall. Fig. 16 shows the divided areas, which are the roof, the left sidewall, the right sidewall, the floor, the front, and the rear of the coach.

Fig. 17 shows the overall source spectrum and the area contributions in different 1/3 octave bands. From Fig. 17, for the dominant 1/3 octave band centered at 250 Hz, its main source was located on the roof. Particularly, in 1/3 octave bands centered from 50 Hz to 125 Hz, the roof had significant contributions of which the average contribution rate reached 40%. In 1/3 octave bands centered above 250 Hz, the contribution rates of the roof and the floor are around 21%, those of the sidewall and the rear are around 17%, and that of the front is only 6%.

4.3 Effect of tunnel on interior noise

4.3.1 Sound pressure overall levels of interior noise in TC01 and TP03

Fig. 18 shows the interior noise levels in TC01 and TP03 running on the ground surface and in a tunnel. The train was running at 300 and 350 km/h, with TC01 being as head car during the measurement. The noise measuring point N6 is under a pantograph, as already stated.

Fig. 15 Noise source identification result at the coach end of TP03 (50–5000 Hz)
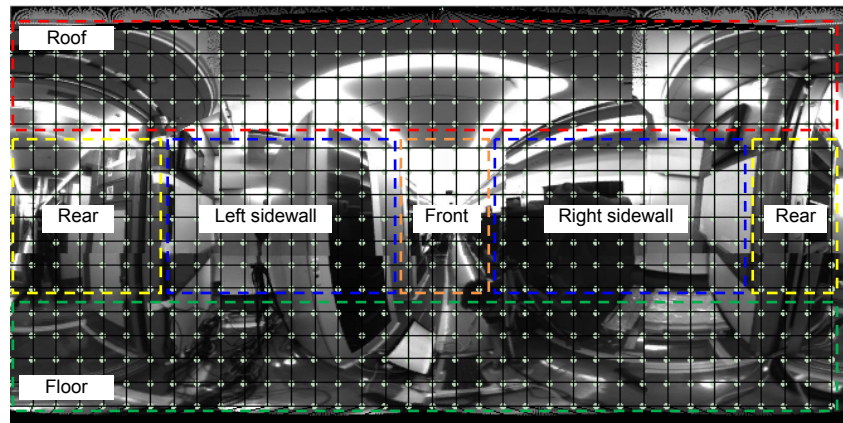
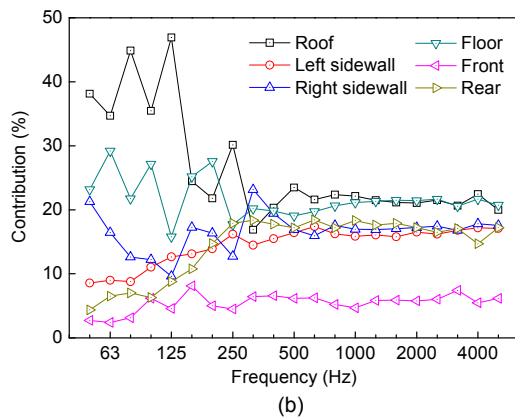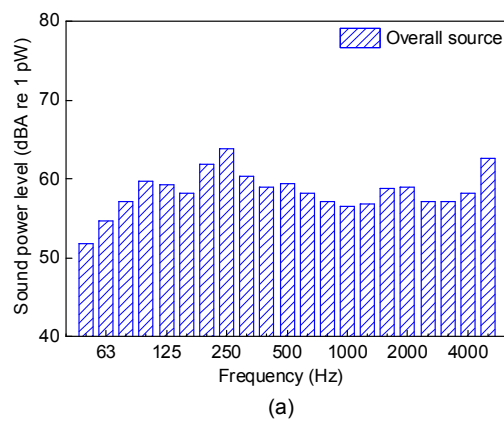**Fig. 16 Divided areas at the coach end of TP03**

(a)

(b)

Fig. 17 Area contributions in 1/3 octave band spectrum at the coach end: (a) overall source spectrum; (b) area contributions in different 1/3 octave bands

Fig. 18 Interior noise levels on different lines

From Fig. 18, when the train was running at 300 and 350 km/h, the interior noise levels in a tunnel are, on average, 8.3 and 6.7 dBA, respectively, higher than those on the ground surface. The data indicate that the ef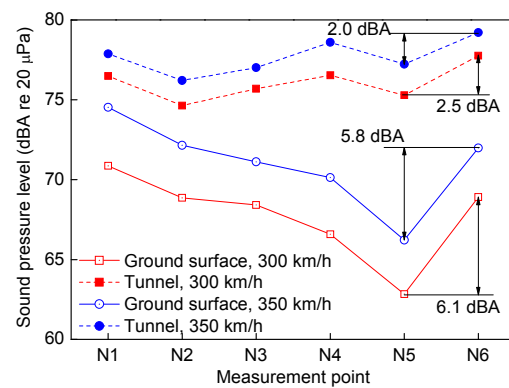fect of the tunnel on interior noise decreases as the train speed increases. An explanation for this is that, the faster the train is, the higher the excitation frequency, the shorter the sound wavelengths, and the weaker the reflected sounds, making the field more like that when the train runs in an open space.

On the ground surface, the interior noises at the end of TP03 are 6.1 and 5.8 dBA higher than those in the middle when the train was running at 300 and 350 km/h, respectively. While in a tunnel, the difference of the interior noises between at the end and in the middle is only about 2 dBA. This is because when the train was running on the ground surface, the main sources are wheel/rail rolling noise and aerodynamic noise which are both dominantly located at the end of the coach. However, when the train was running in a tunnel, the whole coach would be obviously influenced by the mixed sources because the tunnel acts just like a reverberation room.

When on the ground surface, the interior noises in TC01 are higher than those in TP03. However,

when in a tunnel, the interior noises in TC01 are lower than those in TP03. This indicates that running in a tunnel has more influence on the interior noise of a middle coach than that of a head coach.

4.3.2 Frequency spectrum analysis for interior noise of TP03

Fig. 19 shows the noise spectrum in 1/3 octave bands both in the middle and at the end of TP03 at 350 km/h. The left side of the vertical axis indicates the SPLs, and the right side indicates the SPL differences between in a tunnel and on the ground surface.

From Fig. 19, when the train was running in a tunnel at 350 km/h, the interior noise is larger than that on the ground surface in all 1/3 octave bands, especially from 315 Hz to 3150 Hz.

When on the ground surface, the differences of interior noises between in the middle and at the end of the coach are presented in 1/3 octave bands centered above 160 Hz, and their mean difference is 7.8 dBA. In a tunnel, their mean difference is only 3.5 dBA. Therefore, running in a tunnel reduces the differences of interior noise between in the middle and at the end of the coach in mid-high frequency.
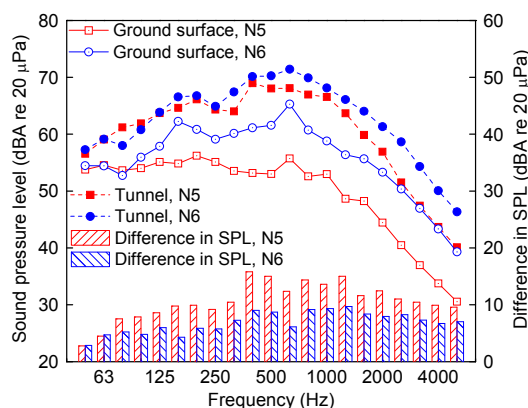

Fig. 19 Interior noise spectrum on different lines at 350 km/h

4.4 Discussion

Because of the limitation of the experimental conditions, only interior noise measurement and noise source identification are carried out. Based on these, the interior noise characteristics of a Chinese high-speed train under several different conditions are preliminarily investigated. Because all the data come from only one high-speed train, conclusions drawn in

this paper can, critically speaking, apply only to trains of the same design, although these conclusions may provide some insights into low-noise design and noise control for other types of trains. Moreover, because of lack of data on exterior noise, vehicle vibrations, and the parameters of the lines, the interior noise mechanism and transfer paths are still to be further studied by more detailed and in-depth work. For low-noise design and noise control of high-speed trains, characteristics analysis of the interior noise is only one of the tasks which have to be carried out. Other tasks include: first, determination of the mechanisms of noise generation, such as wheel/rail rolling noise, aerodynamic noise, and equipment noise (this is because noise reduction is more effective at source); second, identification of the contribution rates of air-borne sound transmission and structure-borne sound transmission from those sources to the vehicle interior. Different transfer paths require different noise reduction measures. Work must be focused on the dominant transfer path.

5 Conclusions

This paper presents an investigation on the characteristics of interior noise of a Chinese high-speed train under a number of typical conditions. The following conclusions can be drawn:

1. Effect of train speed on interior noise: whether TC01 is used as head car or end car, the interior noise characteristics in the VIP cabin are more related to aerodynamic noise. The dominant frequencies of aerodynamic noise affecting the interior noise of the VIP cabin are within 1/3 octave bands centered from 63 Hz to 315 Hz. The main sources are located on the roof and the floor.

2. Effect of track types on interior noise: differences in interior noise between the slab track and the ballast track are train speed-dependent. The higher the speed is, the smaller the difference is. For frequencies lower than 125 Hz, interior noise levels for the ballast track are higher than those for the slab track. However, when frequencies are higher than 500 Hz, the ballast track behaves much better than the slab track. These features are caused by the differences in railpad stiffness and sound absorption between the tracks.

3. Effect of tunnel on interior noise: sound reflections are created when a train runs in a tunnel, increasing interior noise to some extent. The effect of tunnel on the interior noise is more important for the middle coach than that for the head coach. As the train speed increases, the influence (compared with the train running in an open space at the same speed) of running in a tunnel on the interior noise reduces, but only a little. An explanation is that, the faster the train is, the higher the excitation frequency, the shorter the sound wavelengths, and the weaker the reflected sounds, making the field more like that when the train runs in an open space.

Acknowledgments

References

Cohen, I., Benesty, J., Gannot, S., 2010. Speech Processing in Modern Communication: Challenges and Perspectives. Springer Berlin Heidelberg, Germany.
http://dx.doi.org/10.1007/978-3-642-11130-3

Eade, P.W., Hardy, A.E.J., 1977. Railway vehicle internal noise. *Journal of Sound and Vibration*, **51**(3):403-415.
http://dx.doi.org/10.1016/S0022-460X(77)80083-7

Fan, R.P., Su, Z.Q., Meng, G., *et al.*, 2014. Application of sound intensity and partial coherence to identify interior noise sources on the high speed train. *Mechanical Systems and Signal Processing*, **46**(2):481-493.
http://dx.doi.org/10.1016/j.ymssp.2013.11.014

Frémion, N., Vincent, N., Jacob, M., *et al.*, 2000. Aerodynamic noise radiated by the intercoach spacing and the bogie of a high-speed train. *Journal of Sound and Vibration*, **231**(3):577-593.
http://dx.doi.org/10.1006/jsvi.1999.2546

Hardy, A.E.J., 2000. Measurement and assessment of noise within passenger trains. *Journal of Sound and Vibration*, **231**(3):819-829.
http://dx.doi.org/10.1006/jsvi.1999.2565

He, B., Xiao, X.B., Zhou, Q., *et al.*, 2014. Investigation into external noise of a high-speed train at different speeds. *Journal of Zhejiang University-SCIENCE A (Applied Physics & Engineering)*, **15**(12):1019-1033.
http://dx.doi.org/10.1631/jzus.A1400307

Jin, X.S., 2014. Key problems faced in high-speed train operation. *Journal of Zhejiang University-SCIENCE A (Applied Physics & Engineering)*, **15**(12):936-945.
http://dx.doi.org/10.1631/jzus.A1400338

Krylov, V., 2001. Noise and Vibration from High-speed Trains. Thomas Telford, London, UK.

Kuwano, S., Namba, S., Okamoto, T., 2004. Psychological evaluation of sound environment in a compartment of a high-speed train. *Journal of Sound and Vibration*, **277**(3):491-500.
http://dx.doi.org/10.1016/j.jsv.2004.03.010

Létourneaux, F., Guerrand, S., Poisson, F., 2000. Assessment of the acoustical comfort in high-speed trains at the SNCF integration of subjective parameters. *Journal of Sound and Vibration*, **231**(3):839-846.
http://dx.doi.org/10.1006/jsvi.1999.2567

Mauclaire, B., 1990. Noise generated by high speed trains. Proceedings of INTERNOISE.

Mellet, C., Létourneaux, F., Poisson, F., *et al.*, 2006. High speed train noise emission: latest investigation of the aerodynamic/rolling noise contribution. *Journal of Sound and Vibration*, **293**(3-5):535-546.
http://dx.doi.org/10.1016/j.jsv.2005.08.069

Park, B., Jeon, J.Y., Choi, S., *et al.*, 2015. Short-term noise annoyance assessment in passenger compartments of high-speed trains under sudden variation. *Applied Acoustics*, **97**:46-53.
http://dx.doi.org/10.1016/j.apacoust.2015.04.007

Rafaely, B., 2004. Plane-wave decomposition of the sound field on a sphere by spherical convolution. *The Journal of the Acoustical Society of America*, **116**(4):2149-2157.
http://dx.doi.org/10.1121/1.1792643

Sheng, X., Zhong, T., Li, Y., *et al.*, 2017. Vibration and sound radiation of slab high-speed railway tracks subject to a moving harmonic load. *Journal of Sound and Vibration*, **395**:160-186.
http://dx.doi.org/10.1016/j.jsv.2017.02.024

Shin, C.H., Park, W.G., 2003. Numerical study of flow characteristics of the high speed train entering into a tunnel. *Mechanics Research Communications*, **30**(4):287-296.
http://dx.doi.org/10.1016/S0093-6413(03)00025-9

Soeta, Y., Shimokura, R., 2013. Survey of interior noise characteristics in various types of trains. *Applied Acoustics*, **74**(10):1160-1166.
http://dx.doi.org/10.1016/j.apacoust.2013.04.002

Ström, R., 2014. Operational Transfer Path Analysis of Components of a High-speed Train Bogie. MS Thesis, Chalmers University of Technology, Göteborg, Sweden.

Thompson, D.J., Jones, C.J.C., 2000. A review of the modelling of wheel/rail noise generation. *Journal of Sound and Vibration*, **231**(3):519-536.
http://dx.doi.org/10.1006/jsvi.1999.2542

Thompson, D.J., Gautier, P.E., 2006. Review of research into wheel/rail rolling noise reduction. *Proceedings of the Institution of Mechanical Engineers, Part F: Journal of Rail and Rapid Transit*, **220**(4):385-408.
http://dx.doi.org/10.1243/0954409JRRT79

Williams, E.G., 1999. Fourier Acoustics: Sound Radiation and Nearfield Acoustical Holography. Academic Press, New York, USA.

Zhang, J., Han, G.X., Xiao, X.B., *et al.*, 2014. Influence of wheel polygonal wear on interior noise of high-speed

trains. *Journal of Zhejiang University-SCIENCE A (Applied Physics & Engineering)*, **15**(12):1002-1018. http://dx.doi.org/10.1631/jzus.A1400233

Zhang, X.Y., Squicciarini, G., Thompson, D.J., 2016. Sound radiation of a railway rail in close proximity to the ground. *Journal of Sound and Vibration*, **362**:111-124. http://dx.doi.org/10.1016/j.jsv.2015.10.006

中文概要

题　目：不同运行条件下的高速列车车内噪声特性分析

目　的：研究高速列车在不同速度（260~385 km/h）、无砟和有砟轨道以及明线和隧道运行时的车内噪声特性，为高速列车车内减振降噪和车体低噪声设计提供科学依据。

创新点：系统分析高速列车在不同运行条件下的车内噪声总值变化、空间分布、频谱特性和声源贡献，掌握车内噪声随列车运行速度的变化规律、轨道型式和隧道混响对车内噪声的影响，研究轮轨噪声、气动噪声和弓网噪声对车内噪声的作用。

方　法：1.根据不同的列车运行速度，分析车内噪声的变化规律；通过进一步对比头尾车运行时，不同测点位置的噪声总值、显著频率和声源贡献，研究气动作用对车内噪声的影响。2.针对不同轨道型式，分析车内噪声的差异特性；通过进一步对比不同速度下的前、后转向架上方车内噪声测点（其中一个还位于受电弓下方）的噪声总值、显著频率和声源贡献，研究有砟和无砟轨道、弓网噪声对车内噪声的影响以及速度因素的作用。3.对于隧道运行，分析不同速度下在明线和隧道运行时的车内噪声总值和显著频率，研究隧道混响对车内噪声的影响以及速度因素的作用。

结　论：1.TC01车无论作为头车或尾车运行，车内观光区的噪声均主要受气动作用影响。2.随着列车运行速度的提高，轨道型式的不同对车内噪声的影响有所降低。3.隧道混响对中间车的影响要高于头车。

关键词：高速列车；车内噪声；声源识别；贡献分析；不同条件；噪声特性